

SIDEBANDS OF X-RAY DIFFRACTION IN AGE-HARDENED Cu-Ti ALLOY^①

Wei Yinghui, Wang Xiaotian

*School of Materials Science and Engineering,
Xi'an Jiaotong University, Xi'an 710049*

ABSTRACT X-ray diffraction sidebands presented in Cu-Ti alloys have been investigated and sideband profile has been calculated on the basis of the static lattice wave theory. It is concluded that the sideband profile strongly depends on distribution of the modulated wavelength and symmetry of wave form. Diffuse distribution of wavelength is the main reason for sideband moving towards main reflection line, and in this case, the calculated results of the modulated wavelength are not precise by using Daniel-Lipson formula. Moreover, the sideband profile asymmetry is attributed to asymmetry distribution of the modulated wave forms. The calculated sideband profile is in good agreement with the experimental results, which indicates that the static lattice wave theory is successful in dealing with solute atom distribution in solid solution of alloys.

Key words Cu-Ti alloy X-ray diffraction sidebands static lattice wave theory

1 INTRODUCTION

X-ray diffraction sideband is a characteristic of spinodal decomposition taking place in solid solution of alloys. Sidebands in diffraction pattern were discovered in aged Cu-Ni-Fe alloys and interpreted by Daniel and Lipson^[1] in terms of a "wave-like" clustering or periodic redistribution of solute during ageing. Although sideband alongside the main lines is very useful for understanding the process of spinodal decomposition, they are only used to measure wavelength of modulated concentration wave by now. And, there are no detailed investigations on sideband profile and its influence factors. In the paper, an investigation on sideband profile and its influence factors has been conducted by X-ray diffraction experiment and calculation on the basis of the static lattice wave theory in Cu-4% Ti alloy.

2 CALCULATION METHOD OF SIDEBAND PROFILE

The static lattice wave (SLW) theory, which interpreted the coexistence phenomenon of

two solid solution instability mode——spinodal decomposition and ordering, was proposed by Ren and Wang^[2] according to the static concentration and lattice displacement wave theory^[3].

Let us consider a binary solid solution consisting of *A* and *B* atoms. Assuming that $c(\mathbf{r})$ is the occupation probability of finding a solute atom *B* at a crystal lattice site \mathbf{r} , we may expand $c(\mathbf{r})$ in a Fourier series:

$$c(\mathbf{r}) = \sum_{\mathbf{k}} c(\mathbf{k}) \exp[i\mathbf{k} \cdot \mathbf{r}] \quad (1)$$

where \mathbf{k} is the reciprocal vector, $c(\mathbf{r})$ Fourier coefficient of \mathbf{k} wave vector, and $c(\mathbf{k})$ is the amplitude of the static concentration wave. The physical significance of Eq. (1) is that an arbitrary atom distribution in solid solution may be considered as a wave, which is a superposition wave consisting of a series of plane waves with different wave vectors. The plane wave is namely the static concentration wave which is attributed to microcosmic unevenness of the concentration in solid solution.

On the other hand, when a solid solution forms, solvent atoms will diverge ideal site due to atom size difference. Assuming that $\mathbf{R}(\mathbf{r})$ is

① Supported the by National Natural Science Foundation of China

Received Mar. 8, 1996; accepted Jun. 26, 1996

displacement caused by atom size difference at crystal lattice site \mathbf{r} , expand $\mathbf{R}(\mathbf{r})$ in a Fourier series:

$$\mathbf{R}(\mathbf{r}) = \sum_{\mathbf{k}} \mathbf{R}(\mathbf{k}) \exp[i\mathbf{k} \cdot \mathbf{r}] \quad (2)$$

where $\mathbf{R}(\mathbf{k})$ is Fourier coefficient of \mathbf{k} wave vector. Eq. (2)'s physical significance is that an arbitrary lattice displacement distribution may be considered as a wave, which is a superposition wave consisting of a series of plane static lattice displacement waves, and $\mathbf{R}(\mathbf{k})$ is the amplitude of wave vector \mathbf{k} . The plane wave which is attributed to atom's diverging ideal lattice site, is called the static lattice displacement wave.

The above stated is the essentials of the static lattice wave theory.

Assuming that the average concentration of solute B in solid solution AB is \bar{c} . In fact, the atom B in all crystal lattice site distributes unevenly, the occupation probability is a function of the site coordinate \mathbf{r} . Supposing that the occupation probability of B atom at site \mathbf{r} is $c(\mathbf{r})$, that of atom A is $1 - c(\mathbf{r})$, we may obtain atom scattering factors $f(\mathbf{r})$ at site \mathbf{r} :

$$f(\mathbf{r}) = [1 - c(\mathbf{r})]f_A + c(\mathbf{r})f_B \quad (3)$$

where f_A , f_B are atoms scattering factors of A and B atoms respectively.

If \bar{f} is the average of $f(\mathbf{r})$ at all crystal lattice sites, \bar{f} may be written as:

$$\bar{f} = (1 - \bar{c})f_A + \bar{c}f_B$$

It follows from Eq. (3) that:

$$f(\mathbf{r}) = \bar{f} + \Delta f [c(\mathbf{r}) - \bar{c}] \quad (4)$$

where $\Delta f = f_B - f_A$.

Substituting Eq. (1) into Eq. (4) yields:

$$f(\mathbf{r}) = \bar{f} + \Delta f \sum_{\mathbf{k} \neq 0} c(\mathbf{k}) \exp[i\mathbf{k} \cdot \mathbf{r}] \quad (5)$$

Because the solute B is added, an ideal lattice site \mathbf{r} produces displacement $\mathbf{R}(\mathbf{r})$ and turns into the site \mathbf{r}' :

$$\mathbf{r}' = \mathbf{r} + \mathbf{R}(\mathbf{r}) \quad (6)$$

Thus, the crystal diffraction amplitude or structure amplitude may be calculated according to the scattering factor $f(\mathbf{r})$ and displacement $\mathbf{R}(\mathbf{r})$ at every lattice site:

$$Y(\mathbf{q}) = f(\mathbf{r}) \exp[-i\mathbf{q} \cdot \mathbf{r}'] \quad (7)$$

where \mathbf{r}' represents all crystal lattice sites, \mathbf{q} is the amplitude of diffraction wave.

Let $\mathbf{q} = 2\pi(\mathbf{g} + \mathbf{s})$, where \mathbf{g} , which satis-

fies $\mathbf{g} \cdot \mathbf{r} = 1$, is the reciprocal vector of the Bragg reflection, \mathbf{s} the derived reciprocal vector in relation to Bragg position. Substituting Eq. (6) into Eq. (7) yields:

$$Y(\mathbf{q}) = Y_g(\mathbf{s}) = \sum_{\mathbf{r}} f(\mathbf{r}) \exp[-2\pi i \mathbf{s} \cdot \mathbf{r}] \cdot \exp[-2\pi i \mathbf{g} \cdot \mathbf{R}] \quad (8)$$

Generally speaking, $\mathbf{g} \cdot \mathbf{r} \ll 1$. Expanding Eq. (8) in Taylor series and reserving the first and second term. That is:

$$\exp[-2\pi i \mathbf{g} \cdot \mathbf{R}] \approx 1 - 2\pi i \mathbf{g} \cdot \mathbf{R}$$

Thus,

$$Y(\mathbf{q}) = Y_g(\mathbf{s}) = \sum_{\mathbf{r}} f(\mathbf{r}) \cdot (1 - 2\pi i \mathbf{g} \cdot \mathbf{R}) \cdot \exp(-2\pi i \mathbf{s} \cdot \mathbf{r}) \quad (9)$$

As the scattered radiation intensities are proportional to square of scattered wave moduli:

$$I(\mathbf{s}) = |Y_g(\mathbf{s})|^2 \quad (10)$$

Substituting Eq. (9) into Eq. (10) gives:

$$I(\mathbf{s}) = 4 \left| \sum_{\mathbf{r}} f(\mathbf{r}) \cdot \exp[-2\pi i \mathbf{s} \cdot \mathbf{r}] \right|^2 \quad (11)$$

From Eq. (11), one may calculate sideband reflection intensity. It should be noted here that there are various wavelengths and amplitudes of modulation coexisting in the actual modulated structures, and they will have a significant influence on the profile of side bands. Transmission electron microscopic studies of modulated structures in CuTi alloys^[4-6] suggested the coexistence of the modulation with various wavelengths and amplitudes. Therefore, a certain function should be introduced to describe the diffuse periodicity of modulation in calculating reflection intensity.

We consider a crystal structure consisting of N layers, each of which corresponds to one period of the compositional modulation wave. The modulation wave is thought to have a sinusoidal form at an early stage of phase separation and changes its profile gradually to a rectangular form with the development of modulation. Although the profile of modulation wave in actual alloys has no exactly rectangular shape, we assume in the investigation that the profile is rectangular for convenience.

The modulation wave is considered to have X kinds of wavelengths, each of which has Y different wave forms, and consequently contains

totally $(X \cdot Y)$ kinds of wave profiles. Fig. 1 illustrates one of the $(X \cdot Y)$ kinds of wave profiles. A parameter α_Y is introduced to express the symmetry of wave form. It is symmetric when $\alpha_Y = 0.5$ and becomes asymmetric as α_Y doesn't equal 0.5. The dimension of the former half period of the modulation wave is given by $Y \cdot L_x$, where L_x is the Y th wavelength in terms of the number of fcc cells. The amplitude of the modulation wave is assumed to be proportional to L_x and $|c - \bar{c}|$, where \bar{c} is the average composition and $|c - \bar{c}|$ describes the mean amplitude of modulation. And, W_x and P_y are existence probabilities for the X th wavelength and the Y th wave form, respectively.

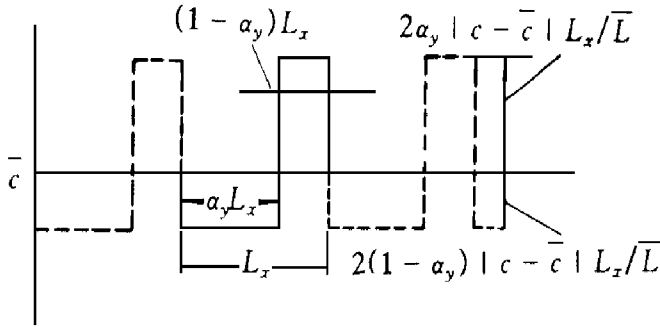


Fig. 1 A kind of modulation wave profile

According to Eq. (11), as the modulation occurs along the $\langle 100 \rangle$ directions in Cu-Ti alloy, the scattered wave amplitude at $(h00)$ in the reciprocal lattice for fcc can be given as follows:

$$Y'_g(s)_{xy} = \bar{f} \cdot \left\{ \sum_{n=0}^{\alpha_Y \cdot L_x - 1} [1 - (1 - \alpha_Y) A_x] \cdot \exp(2\pi i h Z_n / L_x) + \sum_{n=0}^{(1 - \alpha_Y) \cdot L_x - 1} [1 + \alpha_Y \cdot A_x] \cdot \exp(2\pi i h Z'_n / L_x) \right\} \quad (12)$$

$$\text{with } Z_n = n[1 - (1 - \alpha_Y) \cdot B_x] \quad (n = 0, \dots, (\alpha_Y L_x - 1))$$

$$\text{and } Z'_n = (\alpha_Y L_x - 0.5) \cdot [1 - (1 - \alpha_Y) B_x] + (1 + \alpha_Y B_x) / 2 + n' (1 + \alpha_Y B_x) \quad (n' = 0, \dots, [(1 - \alpha_Y) L_x - 1])$$

where \bar{f} is the average atomic scattering factor, A_x the modulation amplitude of scattering factor and B_x one of lattice parameters. A_x and B_x are given by

$$A_x = 2(\bar{f} / \bar{f}) |c - \bar{c}| (L_x / L) \\ B_x = 2\eta |c - \bar{c}| (L_x / L)$$

$$\text{with } \bar{L} = \sum_{x=1}^X W_x L_x$$

where η is the derivative of the lattice parameter, a , with respect to the composition.

We used the values of $f_{Cu} = 20.78$, $f_{Ti} = 13.89^{[7]}$, $\eta = 0.1243 \text{ \AA} \cdot \text{mol}^{-1}$, and $a = 3.6155 \text{ \AA}^{[8]}$. Reflection intensities may be obtained by calculating the structure amplitude factor of each wave and adding their moduli's square together. In order to directly compare with the experimental profiles, the calculated intensity is convoluted by a proper Gaussian distribution and integrated in the reciprocal space to convert to powder diffraction.

3 EXPERIMENTAL DETAILS

The alloys used in this study were prepared by vacuum induction melting of 99.99% purity copper and 99.9% purity titanium. The composition of alloys was found by chemical analysis to be 4% Ti. Also, the alloy contained less than $1.5 \times 10^{-2}\%$ O. The as-cast ingot was swaged to rod and then homogenized in vacuum. The rod was rolled to sheet for electron microscopy. All heat treatment and intermediate anneals were carried out in evacuated titanium gettered quartz capsules. Specimens were solution-treated under vacuum at 1173 K for 2 h and were quenched in an ice brine bath. Aging was carried out either in a fused salt or in a tube furnace with the temperature maintained constant to $\pm 5^\circ\text{C}$. Specimens were encapsulated during ageing except those aged less than 30 min, which were placed directly into the bath or furnace. The aged specimens were cooled rapidly to room temperature by breaking the capsules in water. A Rigaku-C diffractometer equipped with copper target and Ni filter was to record sideband intensity profiles associated with the (200) Bragg reflection. Scanning speed is $0.1^\circ/\text{min}$. An H-800 equipped with a high-angle, double-tilt metallurgical stage was used to observe microstructure.

4 RESULTS AND DISCUSSION

Fig. 2 shows the sideband profiles alongside

the (200) main reflection line in X-ray diffraction pattern of Cu-Ti alloy solution-treated at 1173 K for 1 h, then aged at 673 K for various periods of time. From Fig. 2, it may be seen that: (1) With ageing time prolonged, sidebands move towards the main reflection lines. (2) Diffraction intensities of low-angle and high-angle sidebands are changing with the ageing time. Aged for a short time, intensity of low-angle is high, then low-angle and high-angle tend to be equal in intensities for a prolonged ageing time, and finally the intensity of high-angle sideband is higher than that of low-angle. (3) It is difficult to decide the Bragg angles accurately because the sideband profile is quite diffuse. (4) The intensities of low-angle and high-angle sidebands are asymmetric, the Bragg angle at which sidebands are present is asymmetric, too.

As seen in several studies, the mean wavelength of modulation is usually estimated by

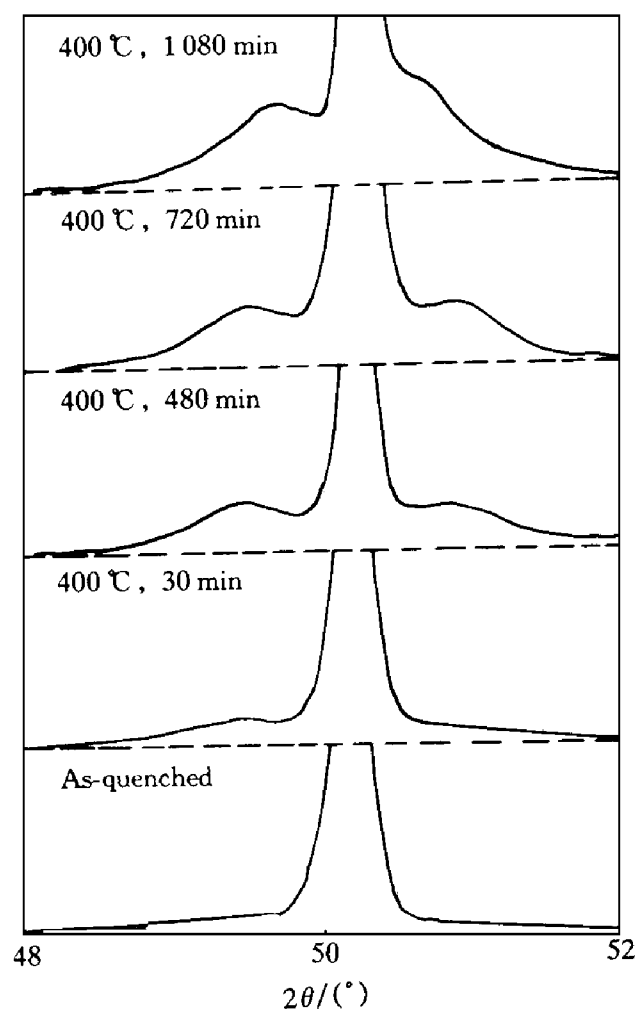


Fig. 2 X-ray sideband profiles around (200) reflection of Cu-4%Ti alloy

using Daniel and Lipson (D-N) formula:

$$L = \frac{h \cdot a_0 \cdot \tan(2\theta)}{(h^2 + k^2 + l^2) \cdot \Delta(2\theta)} \quad (13)$$

where L is the modulation wavelength in terms of the number of unit cells, $\Delta(2\theta)$ the angular displacement of the position between the sideband maximum and the fundamental reflection with hkl and (2θ) the Bragg reflection. However, it is not easy to estimate $\Delta(2\theta)$ accurately because the widths of sidebands are broadened. Even when $\Delta(2\theta)$ can be estimated, it is suggested that the formula does not always give a correct value for the mean wavelength of modulation with a diffuse distribution of wavelength. Fig. 3 shows the dependence of the sideband profile on the wavelength distribution. When the wavelength distribution becomes diffuse, the sidebands are intensified and the maximum position becomes close to the fundamental reflection and the calculated wavelengths deviate the experimental values. The deviation from the true value is seen to increase with the diffuseness of the wavelength distribution. It should be noted that the sideband profile depends strongly on the wavelength distribution. The diffuse distribution of wavelength makes the D-L formula give an incorrect value for the mean wavelength. Such a diffuse distribution may be actually observed at a later stage of ageing. Under the circumstance, the morphology of the modulated structure is even different from that in the early stage of ageing (Fig. 4). What this reflects in the sideband profiles is that the sideband moves toward the main reflection peak with ageing time prolonged.

It is seen that the calculated sideband profile in Fig. 3 is almost symmetric with respect to the fundamental reflection. However, the experimental sideband profile is usually asymmetric at a later stage of ageing. One may obtain the asymmetric sideband profile by alternating the asymmetric factor (Fig. 5). When α_Y equals 0.5, the sideband is symmetric. When α_Y is less than 0.5, the intensity of low-angle sideband is higher. Otherwise, the high-angle one is higher. From this, one sees that the asymmetry of the sideband intensity is attributed to the asymmetry of the modulated wave forms.

At the early stage of spinodal decomposition, solute atoms are clustering in the direction of soft elasticity so that solute-rich and solute-depleted zones are formed. That the solute concentration

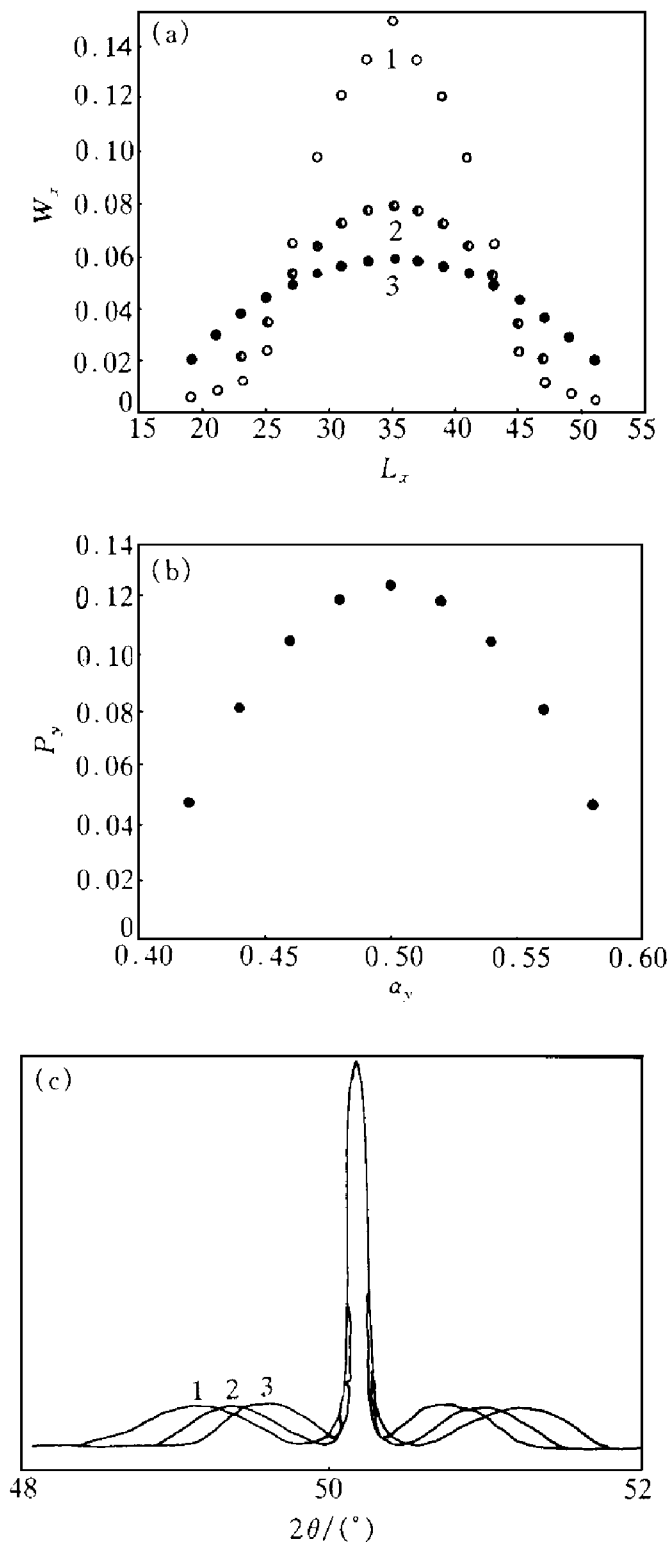


Fig. 3 Dependence of (200) sideband profile on distribution of wavelengths

($X = 17$, $\bar{L} = 35$, $\bar{\alpha} = 0.5$ and $|c - \bar{c}| = 1.7\% \text{ Ti}$)
 (a) —distribution probability of wavelength;
 (b) —distribution probability of asymmetric factor;
 (c) —(200) sideband profile corresponding to (a)

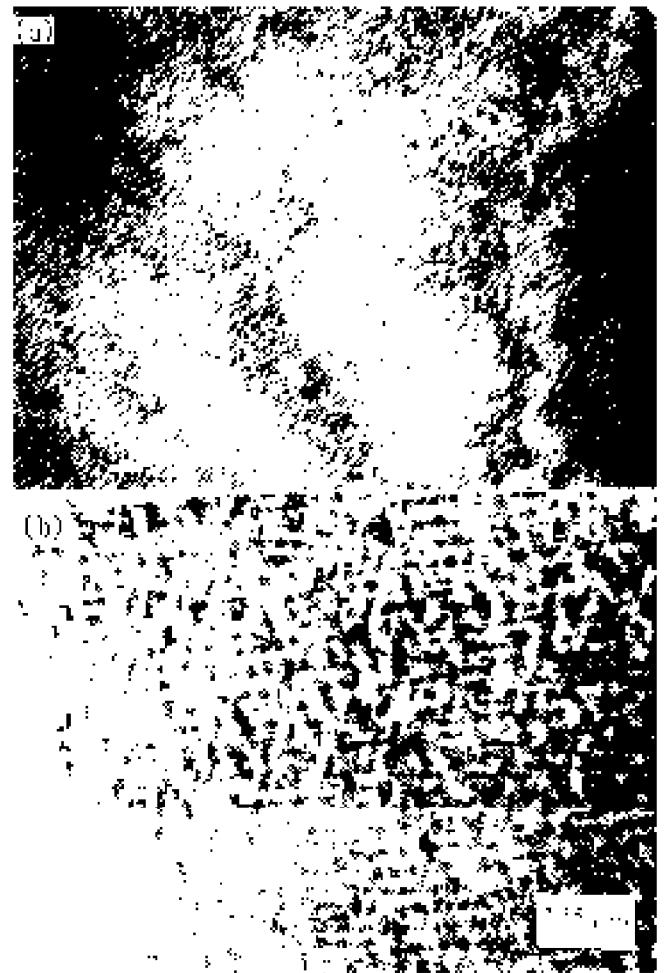


Fig. 4 Electron micrographs of modulated structures in Cu-4%Ti alloy aged at 400 °C

(a) —10 min; (b) —300 min

tration in solute-rich deviates the equilibrium concentration leads to a greater lattice distortion in the zone than that in the solute-depleted zone. Thus, a higher intensity of low-angle sideband caused by the solute-rich zone in X-ray diffraction is present. With the ageing time prolonged, the deviation value of concentration from the equilibrium in solute-rich and solute-depleted zones tends to be equal, that is to say, the concentration wave form is symmetric, the intensities of the high-angle and low-angle sideband gradually become equal. At the later stage of spinodal decomposition, the concentration of the solute-depleted zone is close to that of the matrix, and a metastable equilibrium phase is formed in the solute-rich zone. This leads to that the high-angle sideband approaches the main line and the low-angle sideband no longer moves toward the fundamental reflection and becomes isolated due to a

metastable phase formed. Because the sideband symmetry about the fundamental reflection is poor, it is difficult to calculate the mean wavelength accurately by using D-L formula.

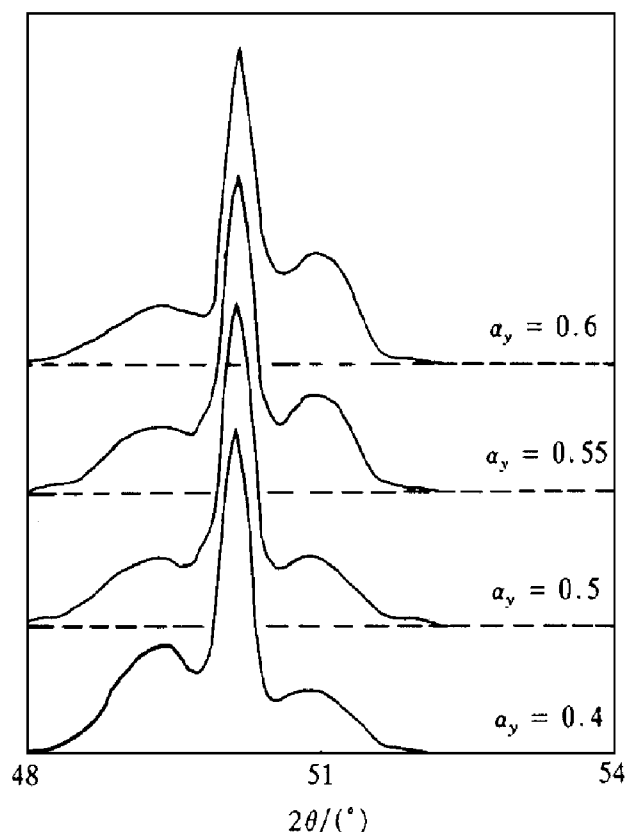
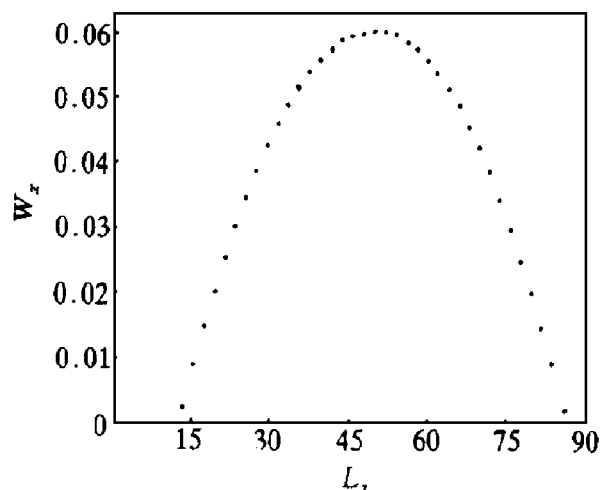


Fig. 5 Dependence of (200) sideband profile on wave form of modulation
($X = 37$, $\bar{L} = 50$, $|c - \bar{c}| = 3.88\%$ Ti)

We calculated the sideband profiles with appropriate values for L_x , α_y , $|c - \bar{c}|$ and distribution for L_x and α_y in order to compare with the experimental one. The calculated sideband profile (Fig. 6) for $x = 41$, $L_x = 55\bar{a}$ (\bar{a} is the

mean lattice parameter), $Y = 13$, $\alpha_y = 0.8$ and $|c - \bar{c}| = 3.6\%$ Ti (mole fraction) is in good agreement with the experimental one as shown in Fig. 1 (aged at 400°C for 1080 min). The mean wavelength for calculation is 261 \AA , but the experimental value is 290 \AA . It suggests that it is inappropriate to calculate the mean wavelength by measuring a deviation of the sideband from the main reflection, 2θ , when a broadened diffuse sideband is present. In order to obtain a true mean wavelength, it is necessary to take a series of photographs in various sight fields and to take the mean.

The distribution of the modulated wavelength, which is sensitive to the ageing temperature, is related to the uneven growth of the modulated structure. When a sample is aged at an elevated temperature, the high-angle sideband merges with the fundamental reflection and the reflection peak from a metastable phase is formed from the low-angle sideband in a short time. Fig. 7 shows the sideband profile of sample which was aged at 500°C for 300 min.

5 CONCLUSIONS

(1) The sidebands alongside the fundamental reflection in X-ray diffraction pattern are attributed to the phase modulation of the periodic change in the lattice parameter.

(2) The asymmetry of the sideband profile is chiefly caused by the asymmetric wave form of the modulated structure.

(3) The uneven distribution of wavelength leads to the sideband's moving toward the fundamental reflection with a prolonged ageing time.

The higher the ageing temperature, the more uneven the distribution of wavelength. Under this circumstance, the D-N formula is inappropriate for calculating the mean wavelength.

(4) The diffuse scattered intensities in the position of deviative Bragg angle, sideband, are calculated by assuming the distribution of solute atoms in the solid solution alloy on the basis of the SLW theory. The calculated results are in good agreement with the experiments.

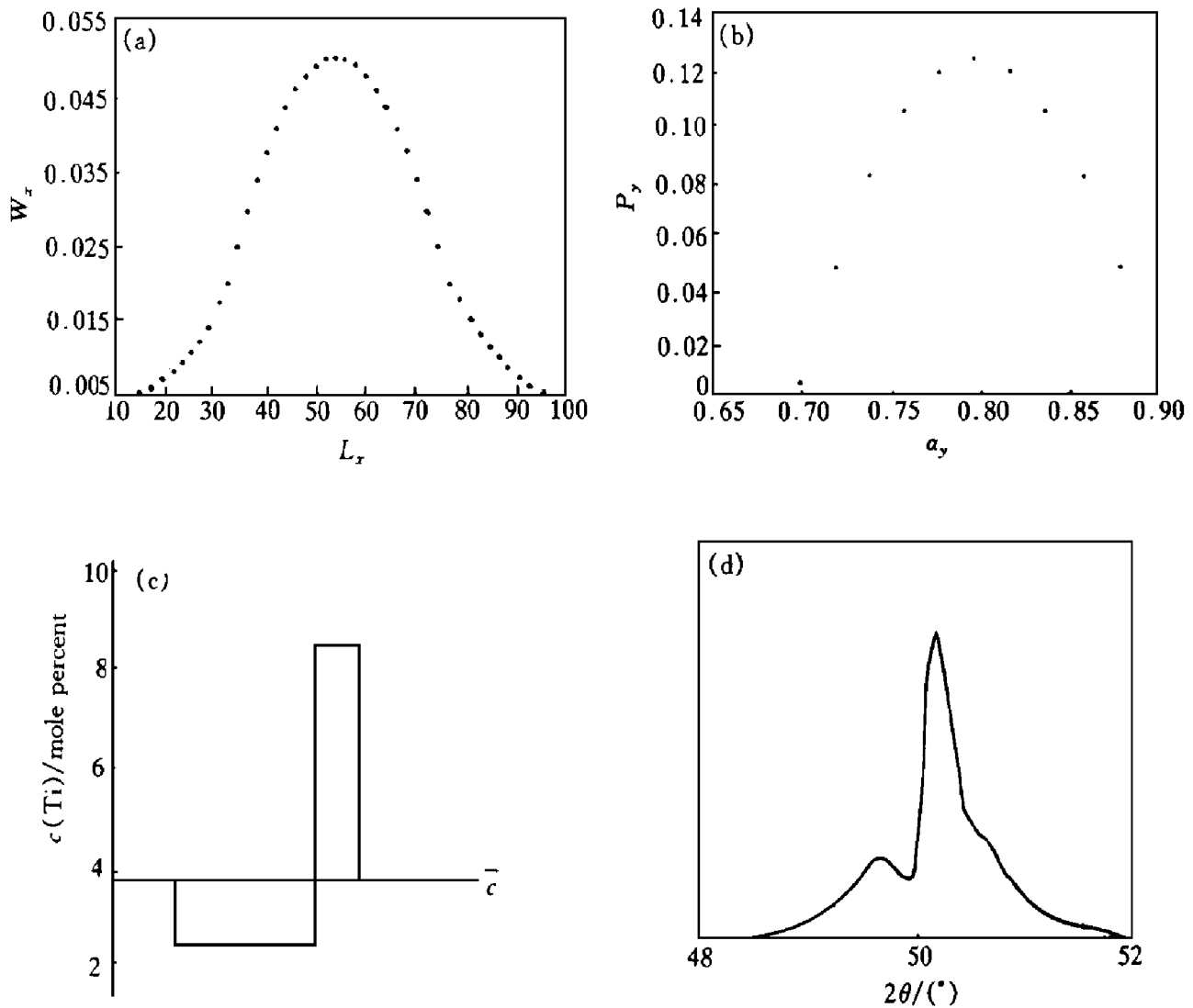


Fig. 6 (200) sideband profiles calculated at subsequent stage of ageing for Cu-4%Ti alloy aged at 400 °C for 1080 min

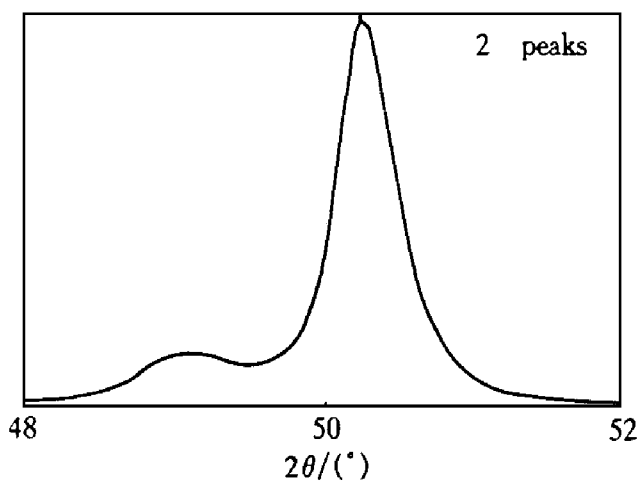


Fig. 7 (200) sideband profiles for Cu-Ti alloy solution-treated at 900 °C for 1 h and aged at 500 °C for 300 min

REFERENCES

- 1 Daniel V, Lipson H. Proc Roy Soc, 1943, A181: 368.
- 2 Ren Xiaobing, Wang Xiaotian. J of Xi'an Jiaotong Univ, (in Chinese), 1994, 28(7): 26.
- 3 Khachaturyan A G. Theory of Structural Transformation Solids. New York: John Wiley & Sons Inc, 1983.
- 4 Cornie J A, Datta A, Soffa W A. Metall Trans, 1973, 4: 727.
- 5 Laughlin D E, Cahn J W. Acta Metall, 1975, 23: 329.
- 6 Datta A, Soffa W A. Acta Metall, 1976, 24: 987.
- 7 Doyle P A, Turnur P S. Acta Cryst, 1968, A24: 390.
- 8 Miyazaki T, Yajima E, Suga H. Trans JIM, 1971, 12: 119-124.

(Edited by Peng Chaoqun)